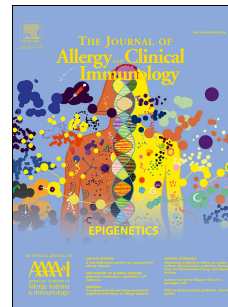


Accepted Manuscript



Human TBK1 is required for early autophagy induction upon HSV1 infection

Liyana Ahmad, PhD, Bayarchimeg Mashbat, PhD, Corwin Leung, MSc, Charlotte Brookes, MSc, Samar Hamad, MSc, Sina Krokowski, MSc, Avinash R. Shenoy, PhD, Lazaro Lorenzo, PhD, Michael Levin, MD, PhD, Peter O'Hare, PhD, Shen-Ying Zhang, MD, PhD, Jean-Laurent Casanova, MD, PhD, Serge Mostowy, PhD, Vanessa Sancho-Shimizu, PhD

PII: S0091-6749(18)31364-2

DOI: [10.1016/j.jaci.2018.09.013](https://doi.org/10.1016/j.jaci.2018.09.013)

Reference: YMAI 13644

To appear in: *Journal of Allergy and Clinical Immunology*

Received Date: 13 November 2017

Revised Date: 28 August 2018

Accepted Date: 7 September 2018

Please cite this article as: Ahmad L, Mashbat B, Leung C, Brookes C, Hamad S, Krokowski S, Shenoy AR, Lorenzo L, Levin M, O'Hare P, Zhang S-Y, Casanova J-L, Mostowy S, Sancho-Shimizu V, Human TBK1 is required for early autophagy induction upon HSV1 infection, *Journal of Allergy and Clinical Immunology* (2018), doi: <https://doi.org/10.1016/j.jaci.2018.09.013>.

This is a PDF file of an unedited manuscript that has been accepted for publication. As a service to our customers we are providing this early version of the manuscript. The manuscript will undergo copyediting, typesetting, and review of the resulting proof before it is published in its final form. Please note that during the production process errors may be discovered which could affect the content, and all legal disclaimers that apply to the journal pertain.

Human TBK1 is required for early autophagy induction upon HSV1 infection

Liyana Ahmad, PhD^a ; Bayarchimeg Mashbat, PhD^b ; Corwin Leung, MSc^a ; Charlotte Brookes, MSc^a ; Samar Hamad, MSc^a ; Sina Krokowski, MSc^{c,d} ; Avinash R. Shenoy, PhD^e , Lazaro Lorenzo, PhD^{f,g} ; Michael Levin, MD, PhD^b ; Peter O'Hare, PhD^a ; Shen-Ying Zhang, MD, PhD^{f,g,h} ; Jean-Laurent Casanova, MD, PhD^{f,g,h,i,j} ; Serge Mostowy, PhD^{c,d} ; Vanessa Sancho-Shimizu, PhD^{a,b*}

^aDepartment of Virology, Division of Medicine, Imperial College London, Norfolk Place, London W2 1PG, UK

^bDepartment of Paediatrics, Division of Medicine, Imperial College London, Norfolk Place, London, W2 1PG, UK

^cMRC Centre of Molecular Bacteriology and Infection (CMBI), Imperial College London, London, SW7 2AZ, UK

^dDepartment of Immunology and Infection, London School of Hygiene and Tropical Medicine, London, WC1E 7HT, UK

^eSection of Microbiology, Medical Research Council Centre for Molecular Bacteriology and Infection, Imperial College London, London, SW7 2AZ, UK.

^fLaboratory of Human Genetics of Infectious Diseases, Necker Branch, INSERM U1163, Paris, France

^gUniversity Paris Descartes, Imagine Institute, Paris, France

^hSt. Giles Laboratory of Human Genetics of Infectious Diseases, Rockefeller Branch, The Rockefeller University, New York, NY, USA

ⁱHoward Hughes Medical Institute, New York, NY, USA

^jPediatric Hematology and Immunology Unit, Necker Hospital for Sick Children, Paris, France

*Corresponding author:

Email: v.sancho-shimizu@imperial.ac.uk

Telephone: +44 02075943914

Address: Department of Paediatrics, Division of Medicine, Imperial College London, Norfolk Place,
London, W2 1PG, UK

Keywords: Autophagy, HSV1, TBK1, TLR, IFN

29 **To the Editor:**

30

31 Mutations disrupting the Toll-like receptor 3 (TLR3)-dependent-interferon (IFN) pathway can underlie
32 herpes simplex encephalitis (HSE) of childhood caused by herpes simplex virus-1 (HSV1) infection. These
33 otherwise healthy HSE patients carry germline mutations in the TLR3-IFN circuit including *TRIF* and *TBK1*^{1, 2}.
34 Their dermal fibroblasts show impaired IFN production following HSV1 infection and poly(I:C) stimulation. A
35 number of these genes (*TLR3*, *TRIF*, *TBK1*) have also been implicated in the process of autophagy. On the other
36 hand, HSV1 is known to antagonize the antiviral IFN pathway and the autophagy machinery in part via TBK1.
37 Specifically, TBK1 is targeted by the viral encoded proteins ICP34.5, ICP27, VP24 and UL46, compromising
38 anti-viral IFN signalling^{3, 4}. In the context of autophagy, TBK1 has been reported to phosphorylate autophagy
39 receptors such as p62 to promote clearance of intracellular pathogens including HSV1 *in vitro*⁵. Herein, we
40 study the role of autophagy in HSV1 infection using dermal fibroblasts from control and HSE patients with
41 autosomal dominant (AD) TBK1 (p.G159A/WT) and autosomal recessive TRIF (p.R141X/R141X) deficiencies.

42

43 Despite showing normal autophagy activation after rapamycin and poly(I:C) stimulation, *TBK1*^{+/-}
44 fibroblasts showed no induction of autophagy following multiple stimuli: cyclic di-guanylate monophosphate
45 (c-di-GMP), HSV1 60mer-dsDNA (60mer-dsDNA), and HSV1 infection. Following rapamycin, LC3B punctate
46 signal increased by 3-fold in both control (media: 20.0%, rapamycin: 72.3%) and *TRIF*^{-/-} (media: 21.8%,
47 rapamycin: 70.0%) fibroblasts, and by 6-fold (media: 11.0%, rapamycin: 61.1%) in *TBK1*^{+/-} fibroblasts,
48 suggesting that TRIF and TBK1 were not required for rapamycin-induced autophagy (Fig 1, A and B). To assess
49 autophagy induced via TLR3, poly(I:C) was used to stimulate fibroblasts leading to a 12-fold (media: 7.1%,
50 poly(I:C): 86.5%) increase of LC3B puncta in control fibroblasts. *TRIF*^{-/-} fibroblasts were unable to induce
51 LC3B puncta, implicating TRIF in poly(I:C)-induced autophagy. *TBK1*^{+/-} fibroblasts however showed a
52 moderate 8-fold (media: 4.0%, poly(I:C): 31.3%) induction of autophagy suggesting its partial role in poly(I:C)-
53 induced autophagy consistent with its partial impairment of poly(I:C)-induced IFN production (Fig 1, A and C)².
54 Although the role of dsRNA-TLR3 pathway in regulating autophagy has been documented in other cell lines, its
55 involvement in infection remains elusive. In addition to TLR3-IFN signaling, TBK1 is also involved in the
56 HSV1 DNA recognition pathway via STING-TBK1-IRF3 which serves to activate type I IFNs, and STING-
57 dependent autophagy^{6, 7}. To evaluate induction of autophagy via this pathway, fibroblasts were transfected with
58 c-di-GMP and 60mer-dsDNA, known to stimulate STING-induced autophagy and IFN production^{6, 7}. Whilst

59 mock treated fibroblasts did not show significant LC3B induction, we observed a 2-fold (c-di-GMP control:
60 20.7%, c-di-GMP: 45.2%) and 1.8-fold (c-di-GMP control: 18.5%, c-di-GMP: 33.6%) increase in punctate
61 LC3B in control and TRIF^{-/-} fibroblasts respectively when transfected with c-di-GMP, compared to the c-di-
62 GMP control. Significant induction of LC3B puncta following 60mer-dsDNA transfection was also observed in
63 control and TRIF^{-/-} fibroblasts by 4-fold (media: 19.6%, 60mer-dsDNA: 84.8%) and 2-fold (media: 28.0%,
64 60mer-dsDNA: 67.6%) respectively. However, c-di-GMP and 60mer-dsDNA stimulation failed to induce LC3B
65 puncta in TBK1^{+/-} fibroblasts (Fig 1, A, D and E) suggesting TBK1 is essential for dsDNA-induced autophagy.

66

67 In control fibroblasts, HSV1 infection triggered a 10-fold (non-infected: 0.2 a.u., infected MOI 5: 1.8
68 a.u.) increase in LC3BII:I and a 2-fold (non-infected: 1.0 a.u., infected MOI 5: 0.5 a.u.) reduction in p62 protein
69 indicating activation of autophagy, as assessed by western blot (Fig 1, F). TRIF^{-/-} fibroblasts also showed a 6-
70 fold (non-infected: 0.2 a.u., infected MOI 5: 1.2 a.u.) LC3BII:I increase following infection at MOI 5. TBK1^{+/-}
71 fibroblasts however showed no change in LC3BII:I or p62 following HSV1 infection suggesting impaired
72 HSV1-induced autophagy. Depletion of endogenous TBK1 using siRNA in control fibroblasts recapitulated this
73 impairment (Fig 1, G). Using immunofluorescence imaging, we found that HSV1 infection triggers two LC3B
74 phenotypes in control fibroblasts: perinuclear LC3B puncta in infected cells and cytoplasmic LC3B puncta in
75 antigen-negative-plaque-neighbouring ('antigen-negative') cells (Fig 2, A). Whilst the former occurs later in
76 infection and is likely the phenomenon termed nuclear develop-derived autophagy (NEDA) as it also stained
77 with LC3A⁸ (Fig 2, A), cytoplasmic LC3B formed early in infection (up to 3 hours post-infection) (Fig 2, B).
78 Strikingly, TBK1^{+/-} fibroblasts failed to form cytoplasmic LC3B puncta in antigen-negative cells, despite being
79 able to form perinuclear LC3B later in infection (Fig 2, A and B). Furthermore, inhibiting TBK1 in control
80 fibroblasts using BX795 resulted in significant reduction in cytoplasmic LC3B formation (see Fig E1 in this
81 article's Online Repository at www.jacionline.org). Whilst the lack of early autophagic induction was specific to
82 TBK1^{+/-} fibroblasts, TRIF^{-/-} fibroblasts only showed delayed induction of autophagy (see Fig E2 in this article's
83 Online Repository at www.jacionline.org), suggesting its partial involvement in HSV1-induced autophagy. The
84 antigen-negative LC3B puncta has been previously reported in HSV1-infected mice trigeminal neurons but was
85 shown to be cGAMP-independent and IFN-dependent⁹. In contrast to this, we find this phenomenon to be
86 TBK1-dependent and IFN β -independent since TRIF^{-/-} fibroblasts, shown to have undetectable IRF3
87 phosphorylation and IFNs after HSV1 infection¹ (see Fig E3, A and E4 in this article's Online Repository at
88 www.jacionline.org), were able to induce this phenotype. Furthermore, IFN treatment was able to induce

89 autophagy in TBK1^{+/-} fibroblasts, ruling out the role of IFN in inducing cytoplasmic LC3B puncta in HSV1
90 infection (see Fig E5 in this article's Online Repository at www.jacionline.org). TBK1^{+/-} fibroblasts also failed
91 to reduce STING following HSV1 infection in contrast to control and TRIF^{-/-} fibroblasts suggesting HSV1
92 induction is STING dependent (see Fig E3, *B*). We confirmed similar HSV1-induced autophagy phenotypes in
93 primary fibroblasts from which these SV40-immortalized cell lines were derived from (see Fig E6 in this
94 article's Online Repository at www.jacionline.org). These results show that the two types of autophagy differ in
95 localization (cytoplasmic vs perinuclear) and temporal response to HSV1 infection, implying that they have
96 different functions. We decided to focus on the TBK1-dependent early cytoplasmic phenotype as the later
97 perinuclear LC3B, likely NEDA, was induced in all cells and has been reported to be a generalized stress
98 response to viral late protein production⁸.

99

100 We next sought to understand how the different triggers of autophagy affect HSV1 infection.
101 Following pre-treatment with poly(I:C), HSV1 replication was significantly reduced in control fibroblasts which
102 can be attributed to the production of IFN β (Fig 2, *C* and *D*). Consistently, with a low dose of HSV1, no viral
103 plaque was observed in control fibroblasts which exhibited cytoplasmic puncta in response to the poly(I:C)
104 treatment (Fig 2, *C*, *D*, *E* and *G*). Interestingly, poly(I:C)-induced LC3B puncta in TBK1^{+/-} fibroblasts was
105 detectable following HSV1 infection. This pre-enhanced autophagy and IFN β production in TBK1^{+/-} fibroblasts
106 however did not improve cell viability or viral replication in contrast to control fibroblasts (Fig 2, *C-G*). TRIF^{-/-}
107 fibroblasts failed to induce autophagy or IFNs following poly(I:C) treatment¹ and hence were not protected
108 against HSV1 infection (Fig 2, *D*). Notably however, cytoplasmic LC3B puncta was present upon HSV1
109 infection of TRIF^{-/-} fibroblasts, confirming that the formation of cytoplasmic LC3B puncta is IFN-independent
110 (Fig 2, *C*, *D* and *G*, Fig E3, *A* and E4). Rapamycin pre-treatment led to the induction of autophagy in control,
111 TRIF^{-/-} and TBK1^{+/-} fibroblasts as expected (Fig 2, *C* and *G*). In control and TRIF^{-/-} fibroblasts, upregulating
112 autophagy using rapamycin prior to HSV1 infection resulted in the same proportion of cytoplasmic LC3B
113 puncta post-infection (non-treated infected vs rapamycin infected) (Fig 2, *C* and *G*). In contrast, rapamycin pre-
114 treated TBK1^{+/-} fibroblasts showed a 4-fold (non-treated infected: 8.7% vs rapamycin-infected: 35.5%) increase
115 of cytoplasmic LC3B puncta in antigen-negative fibroblasts following HSV1 infection (Fig 2, *C* and *G*).
116 Rapamycin pretreatment did not affect viral replication in all cells however it significantly improved cell
117 viability of TBK1^{+/-} cells (non-treated: 55.0% vs rapamycin treated: 76.7%) (Fig 2, *E*, *F* and *G*). Taken together,
118 this shows that rapamycin-induced autophagy selectively increased the number of cytoplasmic LC3B, which

119 confers a cytoprotective effect by increasing cell viability in TBK1^{+/-} fibroblasts. This protective effect of
120 rapamycin could not be attributed to IFN β as rapamycin did not induce IFN β (Fig 2, D).

121

122 In conclusion, we show that in addition to its antiviral role in IFN production via TLR3 and STING^{1,2},
123 ⁶, TBK1 induces autophagy upon HSV1 infection. We demonstrate that TBK1-induced autophagy occurs early
124 during HSV1 infection in antigen-negative fibroblasts, can be mediated by c-di-GMP or HSV1 dsDNA and is
125 TLR3- and IFN-independent. TBK1^{+/-} fibroblasts derived from a HSE patient harboring a dominant negative
126 mutation had a selective impairment of autophagy induction early in infection represented by the lack of
127 cytoplasmic LC3B puncta formation. We believe that host or viral induced factors, possibly acting as danger
128 signals, can trigger autophagy in antigen-negative fibroblasts promoting cell survival without influencing viral
129 replication. This study highlights a possibly cytoprotective role for TBK1 in HSV1-induced autophagy which
130 may serve to control inflammation and has potential implications for patients with HSE.

131

132 *Liyana Ahmad, PhD^a*

133 *Bayarchimeg Mashbat, PhD^b*

134 *Corwin Leung, MSc^a*

135 *Charlotte Brookes, MSc^a*

136 *Samar Hamad, MSc^a*

137 *Sina Krokowski, MSc^{c,d}*

138 *Avinash R. Shenoy, PhD^e*

139 *Lazaro Lorenzo, MSc^{f,g},*

140 *Michael Levin, MD PhD^b*

141 *Peter O'Hare, PhD^a*

142 *Shen-Ying Zhang, MD, PhD^{f,g,h}*

143 *Jean-Laurent Casanova, MD, PhD^{f,g,h,i,j}*

144 *Serge Mostowy, PhD^{c,d}*

145 *Vanessa Sancho-Shimizu, PhD^{a,b*}*

146

147 From ^aDepartment of Virology, Division of Medicine, Imperial College London, Norfolk Place, London W2

148 1PG, UK; ^bDepartment of Paediatrics, Division of Medicine, Imperial College London, Norfolk Place, London

149 W2 1PG, UK; ^cMRC Centre of Molecular Bacteriology and Infection (CMBI), Imperial College London,
150 London, SW7 2AZ, UK; ^dDepartment of Immunology and Infection, London School of Hygiene and Tropical
151 Medicine, London, WC1E 7HT, UK; ^eSection of Microbiology, Medical Research Council Centre for Molecular
152 Bacteriology and Infection, Imperial College London, London, SW7 2AZ, UK; ^fLaboratory of Human Genetics
153 of Infectious Diseases, Necker Branch, INSERM U1163, Paris, France; ^gUniversity Paris Descartes, Imagine
154 Institute, Paris, France; ^hSt. Giles Laboratory of Human Genetics of Infectious Diseases, Rockefeller Branch,
155 The Rockefeller University, New York, NY, USA; ⁱHoward Hughes Medical Institute, New York, NY, USA;
156 ^jPediatric Hematology and Immunology Unit, Necker Hospital for Sick Children, Paris, France.

157

158 *Correspondence: v.sancho-shimizu@imperial.ac.uk

159 LA was supported by the Chancellor's scholarship of Universiti Brunei Darussalam, VSS is a Medical Research
160 Foundation fellow and the work described has been supported by this grant.

161

162 REFERENCES

- 163 1. Sancho-Shimizu V, Pérez de Diego R, Lorenzo L, Halwani R, Alangari A, Israelsson E, et al. Herpes
164 simplex encephalitis in children with autosomal recessive and dominant TRIF deficiency. *J Clin Invest*
165 2011; 121:4889–902.
- 166 2. Herman M, Ciancanelli M, Ou Y-H, Lorenzo L, Klaudel-Dreszler M, Pauwels E, et al. Heterozygous
167 TBK1 mutations impair TLR3 immunity and underlie herpes simplex encephalitis of childhood. *J Exp*
168 *Med* 2012; 209:1567–82.
- 169 3. Verpooten D, Yijie M, Hou S, Yan Z, He B. Control of TANK-binding kinase 1-mediated signaling by
170 the gamma(1)34.5 protein of herpes simplex virus 1. *J Biol Chem* 2009; 284:1097–105.
- 171 4. Zheng C. Evasion of Cytosolic DNA-Stimulated Innate Immune Responses by HSV-1. *J Virol* 2018.
- 172 5. Sparrer KMJ, Gableske S, Zurenski MA, Parker ZM, Full F, Baumgart GJ, et al. TRIM23 mediates
173 virus-induced autophagy via activation of TBK1. *Nat Microbiol* 2017; 2:1543–57.
- 174 6. Burdette DL, Monroe KM, Sotelo-Troha K, Iwig JS, Eckert B, Hyodo M, et al. STING is a direct
175 innate immune sensor of cyclic di-GMP. *Nature* 2011; 478:515–8.
- 176 7. Rasmussen SB, Horan KA, Holm CK, Stranks AJ, Mettenleiter TC, Simon AK, et al. Activation of
177 autophagy by alpha-herpesviruses in myeloid cells is mediated by cytoplasmic viral DNA through a
178 mechanism dependent on stimulator of IFN genes. *J Immunol* 2011; 187:5268–76.

- 179 8. Radtke K, English L, Rondeau C, Leib D, Lippe R, Desjardins M. Inhibition of the host translation
180 shutoff response by herpes simplex virus 1 triggers nuclear envelope-derived autophagy. *J Virol* 2013;
181 87:3990–7.
- 182 9. Katzenell S, Leib DA. Herpes Simplex Virus and Interferon Signaling Induce Novel Autophagic
183 Clusters in Sensory Neurons. *J Virol*. 2016; 90:4706–19.

184

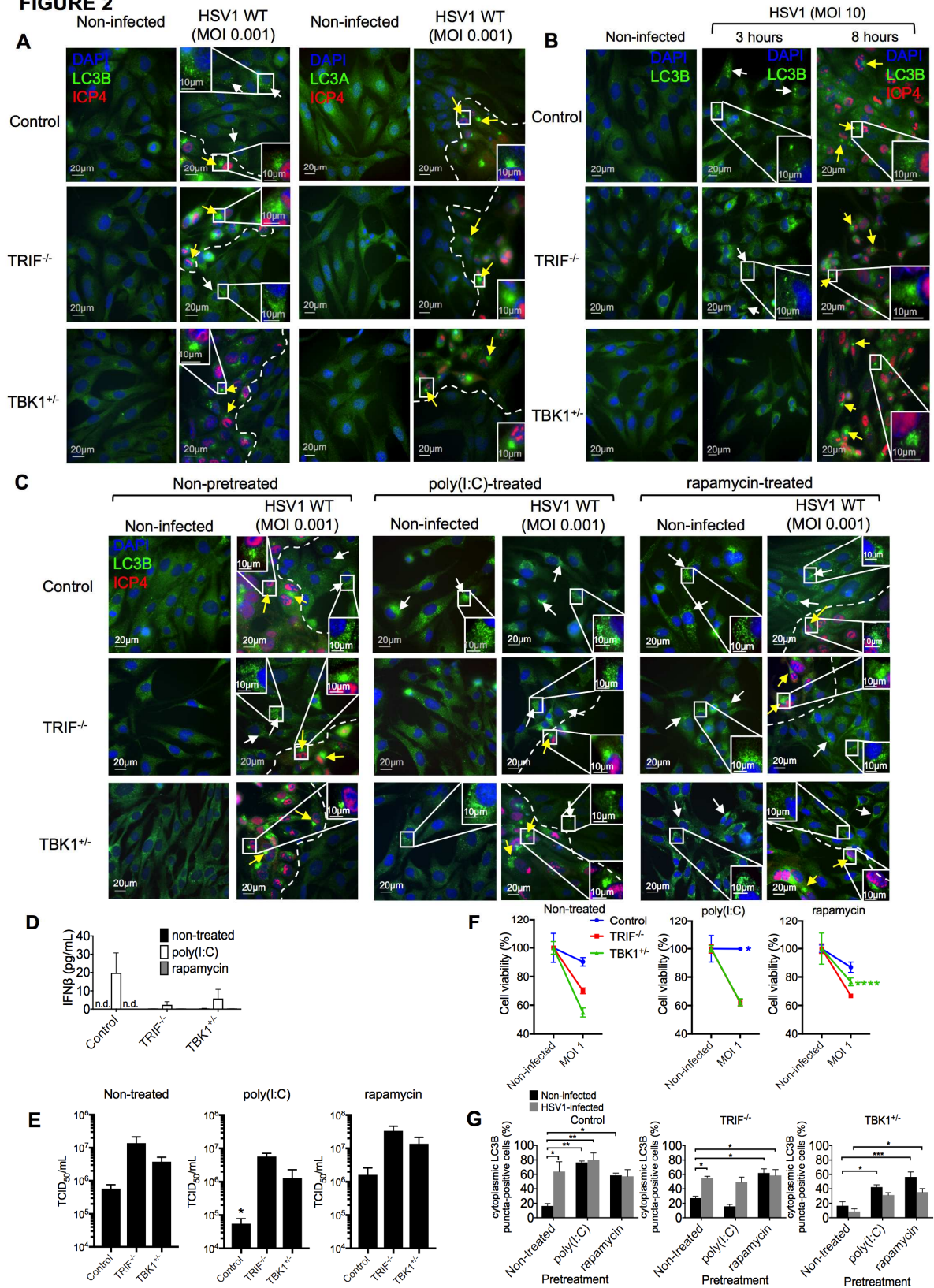
185 **FIGURE LEGENDS**

186 **FIG 1. TBK1^{+/-} fibroblasts show impaired cytosolic-dsDNA- and HSV1-induced autophagy. (A)**
187 Immunofluorescence images of LC3B puncta (green) and DAPI (blue) in fibroblasts. Quantification of LC3B
188 puncta positive fibroblasts stimulated with (B) rapamycin, (C) poly(I:C), (D) cdi-GMP or cdi-GMP control, and
189 (E) 60mer-dsDNA. (F) Immunoblots and densitometric graphs of HSV1-infected fibroblasts. (G) Immunoblot
190 confirming TBK1 siRNA knockdown in control fibroblasts; immunoblots for LC3B, p62, GAPDH in HSV1-
191 infected TBK1 knockdown fibroblasts. Viral titre and immunofluorescence images of infected TBK1
192 knockdown fibroblasts. L; Lipofectamine, (all experiments were performed at least three times; means \pm SEM;
193 **** P <0.0001, *** P <0.001 and * P <0.05).

194

195 **FIG 2. TBK1^{+/-} fibroblasts lack cytoplasmic LC3B puncta induced early in HSV1 infection. (A, B, C)**
196 Immunofluorescence images of fibroblasts stained for HSV1 ICP4 (red), LC3B or LC3A (green), and DAPI
197 (blue). White arrows indicate cytoplasmic LC3B, yellow arrows indicate perinuclear LC3A/B. Dashed lines
198 mark the plaque boundary. (D) IFN β production, (E) viral titre, (F) cell viability and (G) cytoplasmic LC3B
199 puncta positive fibroblasts were quantified. n.d., not-detectable, (n=3; means \pm SEM; **** P <0.0001, *** P
200 <0.001, ** P <0.01 and * P <0.05).

FIGURE 2



1 Legends for Online Repository Figures

2

3 **Fig E1 - TBK1 inhibition reduced cytoplasmic LC3B puncta formation but did not**

4 **affect perinuclear LC3B formation following HSV1 infection (A)** Control and TBK1^{+/-}

5 fibroblasts were pre-treated with 1 μ M of BX795 for 16 hours before infecting with HSV1

6 (MOI 10) for indicated length of time, and being fixed and stained for LC3B (green) and/or

7 ICP4 (red). DAPI (blue) was used the nuclear stain. The scale bar of each representative

8 image is 20 μ m. Inset represents the magnified view of the indicated area and has a scale bar

9 of 10 μ m. White arrows indicate cytoplasmic LC3B, while yellow arrows indicate perinuclear

10 LC3B. **(B)** The percentage of cells positive for cytoplasmic LC3B puncta in (A) was counted

11 on a minimum number of >100 cells. Images are representative of three independent

12 experiments (n=3). Data are represented as mean \pm SEM and were analysed by two-way

13 ANOVA; ** P <0.01.

14

15 **Fig E2 - TRIF^{-/-} fibroblasts showed delayed cytoplasmic LC3B puncta formation – (A)**

16 Fibroblasts grown on coverslips were infected with HSV1 (MOI 10) for indicated lengths of

17 time before being fixed and stained for endogenous LC3B (green) and/or HSV1 ICP4 (red)

18 proteins. DAPI (blue) was used as the nuclear stain. The scale bar of each representative

19 image is 20 μ m. Inset represents the magnified view of the indicated area and has a scale bar

20 of 10 μ m. White arrows indicate cytoplasmic LC3B, while yellow arrows indicate perinuclear

21 LC3B. **(B)** The percentage of cells positive for cytoplasmic LC3B puncta in (A) was counted

22 on a minimum number of >100 cells. Images are representative of three independent

23 experiments (n=3). Data are represented as mean \pm SEM and were analysed by two-way

24 ANOVA; *** P <0.001 and **** P <0.0001.

25

26 **Fig E3 – Endogenous protein levels of TBK1, IRF3, phosphorylated IRF3 and STING**

27 **during HSV1 infection.** Control, TRIF^{-/-} and TBK1^{+/-} fibroblasts were infected with HSV1

28 (MOI 1) for indicated lengths of time. Whole-cell lysates were electrophoresed and probed

29 for endogenous (A) TBK1, IRF3 phosphorylated IRF3 and (B) STING proteins. GAPDH was
30 used a loading control. Relative level of STING to GAPDH was measured by densitometry.

31

32 **Fig E4 – TRIF^{-/-} and TBK1^{+/-} fibroblasts showed impaired IFN β production following**
33 **HSV1 infection.** Control, TRIF^{-/-} and TBK1^{+/-} fibroblasts were infected with HSV1 at
34 indicated MOIs for 24 hours before collecting supernatants and measuring IFN β by ELISA.
35 Data are represented as mean \pm SEM and were analysed by two-way ANOVA; n=3; * P <0.05
36 and **** P <0.0001.

37

38 **Fig E5 - IFN-induced autophagy in fibroblasts** (A) Control, TRIF^{-/-} and TBK1^{+/-} fibroblasts
39 were stimulated with 1×10^5 IU/mL of IFN α -2A for 24 hours before being fixed and stained
40 for endogenous LC3B (green). DAPI (blue) was used as the nuclear stain. The scale bar of
41 each representative image is 20 μ m. Inset represents the magnified view of the indicated area
42 and has a scale bar of 10 μ m. White arrows indicate LC3B puncta. Images are representative
43 of three independent experiments (n=3)

44

45 **Figure E6 - Primary fibroblasts showed similar HSV1-induced autophagy phenotypes to**
46 **SV40-transformed fibroblasts.** Primary fibroblasts grown on coverslips were infected with
47 HSV1 (MOI 10) for 3 or 8 hours before being fixed and stained for endogenous LC3B (green)
48 and/or HSV1 ICP4 (red) proteins. DAPI (blue) was used as the nuclear stain. The scale bar of
49 each representative image is 20 μ m. Inset represents the magnified view of the indicated area
50 and has a scale bar of 10 μ m. White arrows indicate cytoplasmic LC3B, while yellow arrows
51 indicate perinuclear LC3B. Images are representative of three independent experiments
52 (n=3).

1 METHODS

2

3 *Cell lines*

4 Human SV40-immortalized dermal fibroblasts from healthy control, TBK1^{+/-} (p.G159A), TRIF^{-/-}
5 patients^{E1, E2}, and Vero (African green monkey kidney) cells were maintained in 5% CO₂ incubator at
6 37°C in DMEM supplemented with 10% fetal bovine serum (FBS).

7

8 *Viral infection and quantification*

9 Human fibroblasts were infected with HSV1-GFP (KOS strain with GFP-tagged capsid protein VP26)
10 or HSV1 (strain 17AR+) at various MOIs and timepoints for immunoblot and immunofluorescence
11 experiments. After 1 hour infection in DMEM supplemented with 2% FBS, the virus was removed and
12 new media added with 1% HSV1 human neutralizing antibody. Viral titres were determined by
13 infecting a confluent monolayer of Vero cells in a 12-well or 96-well plate, and performing plaque
14 assay on them or calculating the 50% end point (TCID₅₀/mL)^{E3}.

15

16 *Stimulation and treatments*

17 Fibroblasts cells were stimulated with 25 µg/mL of poly(I:C) (GE Healthcare), 10 nM of rapamycin
18 (Calbiochem) or 1X10⁵ IU/mL of IFNα-2A (PBL Assay Science) for 24 hours, or treated with 1µM of
19 TBK1 inhibitor BX795^{E4} (Sigma) for 16 hours, or transfected with 8 µg/mL of c-di-GMP (Invivogen)
20 or c-di-GMP control (Invivogen) for 2 hours, or 2 µg/mL of HSV1 dsDNA (60mer sequence: 5'-
21 TAAGACACGATGCGATAAAATCTGTTTGTAAAATTTATTAAGGGTACAAATTGCCCTAGC-
22 3'; Integrated DNA Technology) for 3 hours. C-di-GMP, c-di-GMP control and HSV1 dsDNA were
23 delivered by Lipofectamine® 2000 (L) transfection. For pre-treatment experiments, fibroblast were
24 incubated with either rapamycin or poly(I:C) for 16 hours before infecting with HSV1.

25

26 *Cell viability assay*

27 Cells were plated in a flat-bottomed 96-well plate in triplicates at a density of 0.18X10⁶ cells/mL in
28 10% FBS-supplemented DMEM. Fibroblasts were pre-treated for 16 hours before being infected with
29 HSV1 MOI of 1 for 24 hours. The viability of fibroblasts was measured using CellTiter 96® AQueous

30 Non-Radioactive Cell Proliferation Assay (MTS) kit (Promega) and performed as per manufacturer's
31 instructions. Cell viability was determined by normalizing to non-infected cells of each cell line.

32

33 *RNA interference*

34 Cells were seeded in 10% FBS-supplemented DMEM at 0.05×10^6 cells/well in a flat-bottomed 24-well
35 plate and incubated for 18 hours in 37°C humidified incubator. Medium was then replaced with fresh
36 2% FBS-supplemented DMEM and cells were transfected with 15 nM of scramble (siNegative)
37 (Ambion) or pooled three TBK1-specific (siTBK1) small interfering RNAs (siRNAs) (siRNA ID no.
38 134003, 134002 & 899, Ambion) at 80% confluency using Lipofectamine® RNAiMAX vector (Life
39 Technologies) and incubated for further 48 hours in 37 °C incubator.

40

41 *Immunofluorescence and quantification of puncta-positive cells*

42 Cells were grown at 50% confluency on 13 mm diameter coverslips and fixed with 100% methanol on
43 ice, before washing them with 1X phosphate buffered saline (PBS). Blocking was done in 10%-FBS
44 PBS and cells were permeabilized with 0.1% TritonX-100 in PBS. Staining was done in a moist
45 chamber using the following antibodies: LC3B (1:500 dilution, Abcam), cleaved LC3A (1:100
46 dilution, Stratech), HSV1 immediate early protein ICP4 (clone 10F1) (1:500 dilution, Virusys), Alexa
47 Fluor-488 and -594 conjugated secondary antibodies (1:750 and 1:1000 dilutions respectively, Life
48 Technologies). Images were taken with 63X oil-immersion lens on a widefield fluorescence
49 microscope (Zeiss Axio Observer). The number of LC3B puncta-positive cells was quantified on a
50 minimum number of 100 cells per experiment.

51

52 *Immunoblotting*

53 Whole-cell lysates of fibroblasts infected with HSV1 for 48 hours were harvested in 1X Laemmli
54 buffer supplemented with protease inhibitor cocktail (Roche), 10% β-mercaptoethanol and 1:1000 of
55 benzamide hydrochloride (Sigma). Lysates were denatured and electrophoresed on 12% tris-glycine or 10%
56 bis-tris gels (Biorad). Proteins were transferred onto PVDF membrane (Invitrogen), probed with
57 primary and secondary horse-radish peroxidase (HRP)-conjugated antibodies (1:1000 and 1:10,000
58 dilution respectively) and subsequently detected using enzyme-chemiluminescent reagents (GE
59 Healthcare). For LC3B immunoblots, bafilomycin A1 (Sigma) was added to culture medium for 6

60 hours prior to lysis for immunoblotting to block LC3BII recycling to LC3BI. The following antibodies
61 were used for immunoblotting: LC3B (Cell Signaling Technology), p62 (MBL International), TBK1
62 (Cell Signaling Technology), IRF3 (D83B9) (Cell Signaling Technology), IRF3-phospho (S396) (Cell
63 Signaling Technology), STING (D2P2F) (Cell Signaling Technology), and GAPDH-HRP (Santa Cruz
64 Biotech). GAPDH was used as a loading control.

65

66 *ELISA*

67 IFN β secretion in recovered supernatants of cells pre-treated with rapamycin or poly(I:C) for 24 hours
68 was measured using the VeriKine-HSTM human IFN β serum ELISA kit (assay range: 1.2 – 150 pg/mL)
69 (PBL Assay Science) following the manufacturer's instructions.

70

71 *Statistical analysis and software*

72 Immunofluorescence images were analysed by Icy software. Densitometric analyses of immunoblots
73 were carried out using ImageJ. Statistical significance was assessed by two-way ANOVA using Prism
74 7 (Graphpad) software. Number of fluorescent cells or LC3B puncta-positive cells was quantified using
75 ImageJ software. All experiments were performed at least 3 times.

76

77 REFERENCES

78 E1. Sancho-Shimizu V, Pérez de Diego R, Lorenzo L, Halwani R, Alangari A, Israelsson E, et al.
79 Herpes simplex encephalitis in children with autosomal recessive and dominant TRIF deficiency. J
80 Clin Invest 2011;121:4889–902.

81 E2. Herman M, Ciancanelli M, Ou Y-H, Lorenzo L, Klaudel-Dreszler M, Pauwels E, et al.
82 Heterozygous TBK1 mutations impair TLR3 immunity and underlie herpes simplex encephalitis of
83 childhood. J Exp Med 2012;209:1567–82.

84 E3. Reed LJ, Muench H. A simple method of estimating fifty per cent endpoints. Am J
85 Hyg. 1938;27:493–497.

86 E4. Clark K, Plater L, Peggie M, Cohen P. Use of the pharmacological inhibitor BX795 to study the
87 regulation and physiological roles of TBK1 and IkappaB kinase epsilon: a distinct upstream kinase
88 mediates Ser-172 phosphorylation and activation. J Biol Chem. 2009;284:14136–46.

Fig E1

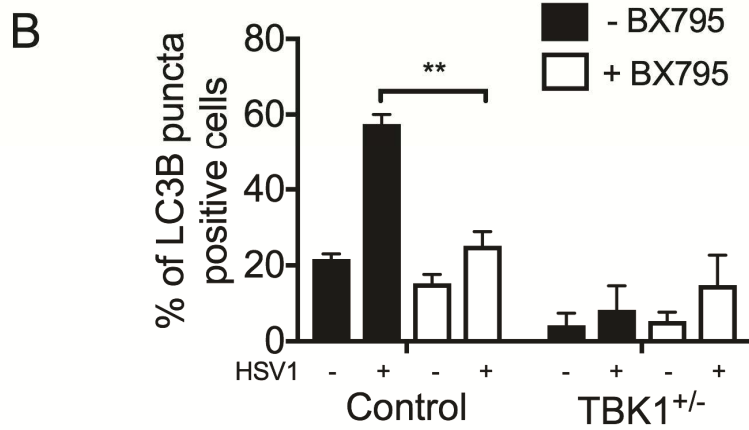
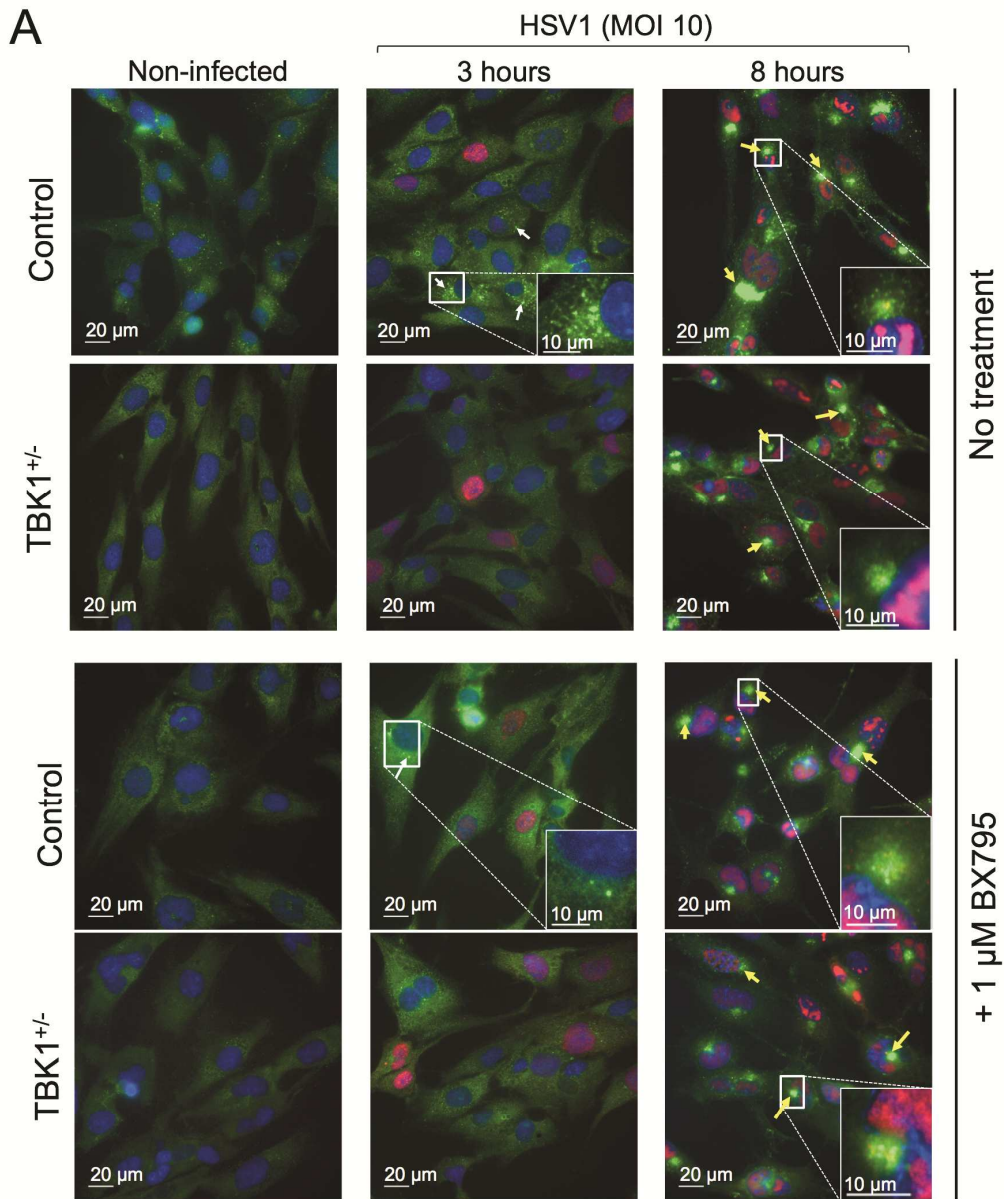


Fig E2

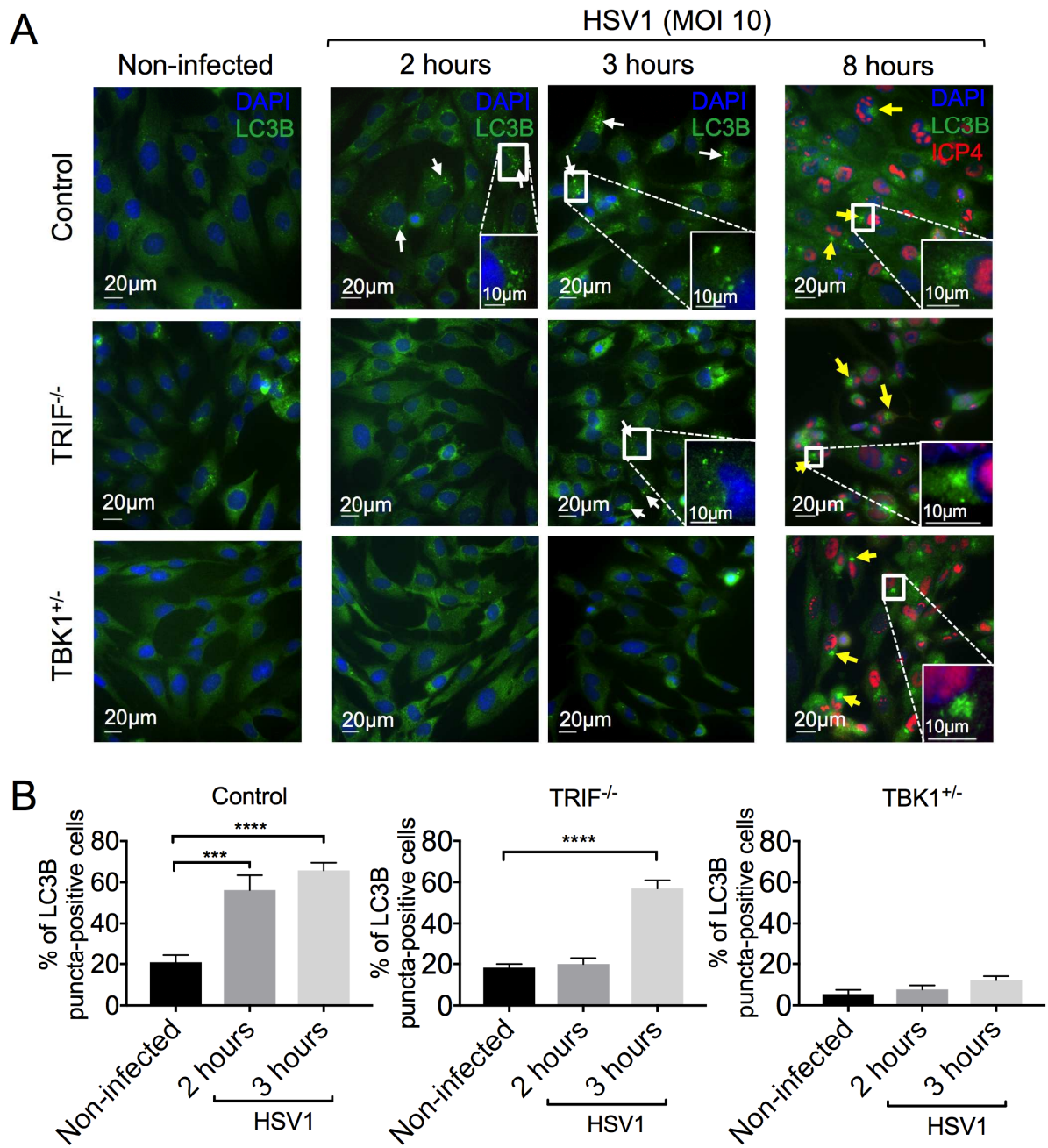


Fig E3

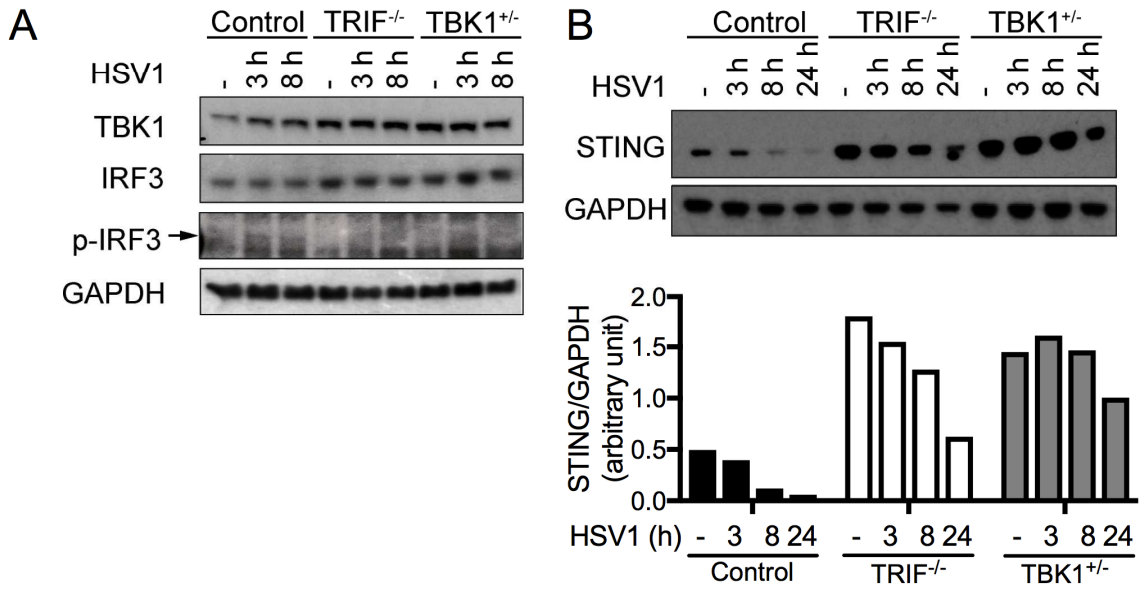


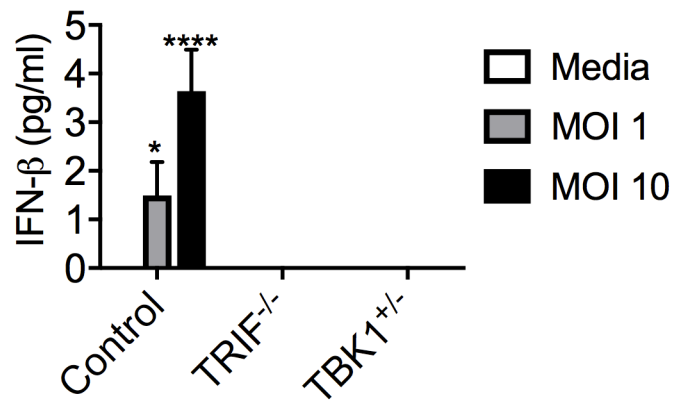
Fig E4

Fig E5